

Gravity currents in unstably stratified fluids

Chenyue XIE, Xiangming XIONG, Jianjun TAO *

CAPT-HEDPS, SKLTCS, Department of Mechanics and Engineering Science,
College of Engineering, Peking University, Beijing 100871, China

(Received / Revised)

January 14, 2022

Abstract

The effects of unstably stratification on the two-dimensional gravity current are studied theoretically and numerically during the slumping phase in this paper. By expanding Benjamin's inviscid theory from homogeneous fluids to stratified fluids, it is shown that the current front speed decreases when the current fluid and the ambient medium are unstably stratified. Though the density interface mixing occurs, the relations among the front speed, the front height, and the stratification parameters predicted by the present inviscid theory agree well with the numerical simulations of lock-exchange gravity currents with different initial lock heights, and the underlying mechanism for this agreement is explained in terms of the current properties.

Key words gravity current, front speed, unstable stratification

1 Introduction

The gravity current, which refers to the propagation of a fluid into an ambient fluid with a different density^[1,2], has been extensively studied analytically, numerically, and experimentally due to its importance in geophysics, atmospheric physics, and environmental fluid mechanics^[3-5]. The gravity current undergoes three propagation stages: the acceleration stage, the slumping stage, and the self-similar deceleration stage. The front speed of the gravity current at the slumping stage is almost constant and has been studied in the non-Boussinesq currents^[6], the partial-depth gravity currents^[7], and the intrusive gravity currents^[8]. By assuming that both fluids are homogeneous and inviscid^[1], a steady theory was developed first by Benjamin for two essential parameters of the current, the front speed and

*Corresponding author, E-mail: jjtao@pku.edu.cn

the current height, and was extended for stably stratified ambient fluids with linear^[9] and nonlinear^[10] density profiles, where the front speeds were found to be smaller than their counterparts in homogeneous ambient fluids. The dissipationless conjugate-state solutions of the steady theory^[10] are consistent with the experimental results of boundary gravity currents^[11] and intrusive gravity currents^[12, 13]. An alternative vorticity-based steady model was proposed^[14] and extended to consider Boussinesq gravity currents in sheared and stably stratified ambient fluids^[15, 16] and non-Boussinesq gravity currents^[17]. Homogeneous and stably stratified gravity currents and intrusive gravity currents in stably stratified ambient fluids have been studied as well with one-layer shallow-water models^[18–22]. Because the thermal capacities of sand and earth are generally smaller than that of the air, their temperature increases faster than that of the surrounding air under the sunshine, and hence the lower part of the atmosphere may illustrate inverse or unstable stratification (denser fluid lies higher) in sunny days. It is also known that the atmosphere is unstably stratified in the troposphere, and the unstable stratification results in a richer set of convection behaviors, such as the significant atmosphere mixing and the transport of sand and dust^[23, 24]. Though various theoretical models have been proposed in the literature for the gravity currents, the corresponding study for currents in unstably stratified ambient fluids is still rudimental, and this is the main motivation of the present paper.

2 Physical model and inviscid theory

A schematic plot of the gravity current between two stratified fluids in a horizontal channel is shown in Fig. 1. In the coordinate system moving at the front speed U , the origin O is the stagnation point at the bottom boundary. The coordinates in the horizontal and vertical directions are x and z , respectively. The density profiles in the far upstream ambient fluid and the far downstream current are $\rho_a(z)$ and $\rho_c(z)$, respectively.

When the density difference between the two fluids is small, the two-dimensional Navier-Stokes equations with the Boussinesq approximation are

$$\frac{\partial u}{\partial x} + \frac{\partial w}{\partial z} = 0, \quad (1)$$

$$\frac{\partial u}{\partial t} + u \frac{\partial u}{\partial x} + w \frac{\partial u}{\partial z} = -\frac{1}{\rho_0} \frac{\partial p}{\partial x} + \nu \nabla^2 u, \quad (2)$$

$$\frac{\partial w}{\partial t} + u \frac{\partial w}{\partial x} + w \frac{\partial w}{\partial z} = -\frac{1}{\rho_0} \frac{\partial p}{\partial z} - \frac{\rho}{\rho_0} g + \nu \nabla^2 w, \quad (3)$$

$$\frac{\partial \rho}{\partial t} + u \frac{\partial \rho}{\partial x} + w \frac{\partial \rho}{\partial z} = \kappa \nabla^2 \rho, \quad (4)$$

where (u, w) , ρ , and p are the velocity, density, and pressure of the fluids, respectively. t is the time. g is the magnitude of the gravitational acceleration. ν and κ are the kinematic viscosity and the density diffusion coefficient of the fluids. ρ_0 is a reference density and will be prescribed later.

The minimum density in the unstably stratified ambient fluid is $\rho_B = \rho_a(0)$, which is the density of the far upstream ambient fluid at the bottom boundary. The maximum density in the unstably stratified current is $\rho_M = \rho_c(h)$, where h is the height of the gravity current. The stratification parameters in the ambient

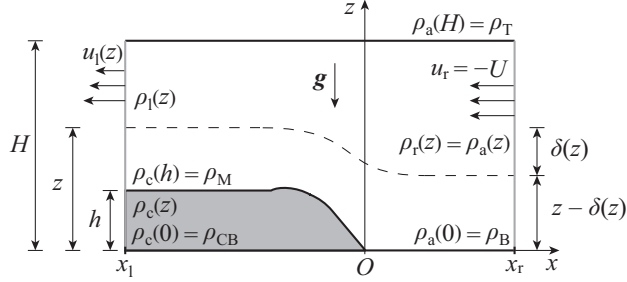


Figure 1: A schematic plot of the gravity current in the reference frame moving with the current front. The shaded region represents the current. The dashed line is a representative streamline.

fluid and the current are defined as

$$S = \frac{\rho_T - \rho_B}{\rho_M - \rho_B} = \frac{\rho_a(H) - \rho_a(0)}{\rho_c(h) - \rho_a(0)}, \quad (5)$$

$$\sigma = \frac{\rho_M - \rho_{CB}}{\rho_M - \rho_B} = \frac{\rho_c(h) - \rho_c(0)}{\rho_c(h) - \rho_a(0)}, \quad (6)$$

respectively. Here, $\rho_T = \rho_a(H)$ is the density of the far upstream ambient fluid at the top boundary, and $\rho_{CB} = \rho_c(0)$ is the density of the far downstream current at the bottom boundary. Note that the downstream side is in the $-x$ direction. In this paper, we only consider the cases with $\rho_M \geq \rho_T$ and $\rho_{CB} \geq \rho_B$. Consequently, the difference between the maximum density in the current and the minimum density in the ambient fluid ($\rho_M - \rho_B$) is the maximum density variation in the present configuration. Homogeneous and unstably stratified ambient fluids correspond to $S = 0$ and $0 < S \leq 1$, respectively. Homogeneous and unstably stratified currents correspond to $\sigma = 0$ and $0 < \sigma \leq 1$, respectively.

The Froude number is defined as

$$Fr = \frac{U}{\sqrt{g'h}}, \quad (7)$$

where the reduced gravity g' is defined as

$$g' = \epsilon g, \quad (8)$$

$$\epsilon = \frac{\rho_M - \rho_B}{\rho_0} \ll 1. \quad (9)$$

The unstable stratification means that the denser fluid lies above the lighter fluid, but does not necessarily mean that the Rayleigh-Bénard type instability will occur. It is known that Rayleigh-Bénard convection will not happen when the unstable stratification is weak and the Rayleigh number is less than a threshold value. In this paper, the unstable stratifications are not strong ($\epsilon \ll 1$) and finite periods of the slumping phase exist for all test cases.

Following Benjamin's theory^[1] and its extensions^[9,10], the gravity current at the slumping stage is assumed to be steady, and the momentum and the density

diffusions are ignored ($\nu = 0$ and $\kappa = 0$). Consequently, Eqs. (2)–(4) are simplified as

$$u \frac{\partial u}{\partial x} + w \frac{\partial u}{\partial z} = -\frac{1}{\rho_0} \frac{\partial p}{\partial x}, \quad (10)$$

$$u \frac{\partial w}{\partial x} + w \frac{\partial w}{\partial z} = -\frac{1}{\rho_0} \frac{\partial p}{\partial z} - \frac{\rho}{\rho_0} g, \quad (11)$$

$$u \frac{\partial \rho}{\partial x} + w \frac{\partial \rho}{\partial z} = 0. \quad (12)$$

At the bottom and top walls, we assume the no-penetration boundary conditions:

$$w|_{z=0} = w|_{z=H} = 0. \quad (13)$$

In the far downstream region, it is assumed that the current height h is constant, the heavier fluid is static, and the ambient fluid flow is unidirectional. In the far upstream ambient fluid, the flow is assumed to be uniform. The following boundary conditions are used for the flow shown in Fig. 1:

$$\rho_1(z) \equiv \rho(x_1, z) = \rho_c(z), \quad 0 \leq z < h, \quad (14)$$

$$u_1(z) \equiv u(x_1, z) = 0, \quad 0 \leq z < h, \quad (15)$$

$$w(x_1, z) = \frac{\partial w}{\partial x}(x_1, z) = 0, \quad 0 \leq z \leq H, \quad (16)$$

$$\rho_r(z) \equiv \rho(x_r, z) = \rho_a(z), \quad 0 \leq z \leq H, \quad (17)$$

$$u_r(z) \equiv u(x_r, z) = -U, \quad 0 \leq z \leq H, \quad (18)$$

$$w(x_r, z) = \frac{\partial w}{\partial x}(x_r, z) = 0, \quad 0 \leq z \leq H, \quad (19)$$

where x_1 and x_r are assumed to be a far downstream position and a far upstream position, respectively. The expressions of the density and velocity in the far downstream ambient fluid are derived in Appendix A, and the main results are

$$\rho_1(z) \equiv \rho(x_1, z) = \rho_a(z - \delta(z)), \quad h < z \leq H \quad (20)$$

$$u_1(z) \equiv u(x_1, z) = -U[1 - \delta'(z)], \quad h < z \leq H, \quad (21)$$

where $\delta(z)$ is the streamline displacement (Fig. 1) and satisfies

$$\delta''(z) = \frac{g}{\rho_0 U^2} \frac{d\rho_a}{dz} \Big|_{z-\delta(z)} \delta(z), \quad h < z \leq H, \quad (22)$$

$$\delta(h) = h, \quad (23)$$

$$\delta(H) = 0. \quad (24)$$

Here, $\delta' \equiv d\delta/dz$ and $\delta'' \equiv d^2\delta/dz^2$.

Next, we derive the relationship between the front speed U and the current height h from the momentum equations. Integrating Eq. (11) from $(x_r, 0)$ to (x_r, z) and using Eqs. (17) and (19), we have

$$p_r(z) \equiv p(x_r, z) = p_r(0) - g \int_0^z \rho_a(z') dz', \quad 0 \leq z \leq H. \quad (25)$$

Integrating Eq. (10) from $(x_1, 0)$ to $(x_r, 0)$ and using Eqs. (13), (15), and (18), we have

$$p(x_1, 0) = p(x_r, 0) + \frac{1}{2} \rho_0 U^2. \quad (26)$$

Integrating Eq. (11) from $(x_1, 0)$ to (x_1, z) and using Eqs. (16) and (26), we have

$$p_1(z) \equiv p(x_1, z) = p_r(0) + \frac{1}{2}\rho_0 U^2 - g \int_0^z \rho_1(z') dz', \quad 0 \leq z \leq H. \quad (27)$$

Integrating Eq. (10) in the region $[x_1, x_r] \times [0, H]$ and using Eqs. (1) and (13), we have

$$\int_0^H (p_1 + \rho_0 u_1^2) dz = \int_0^H (p_r + \rho_0 u_r^2) dz. \quad (28)$$

Substituting Eqs. (14)–(21), (25), and (27) into Eq. (28) and using Eqs. (22)–(24), we have

$$\begin{aligned} 0 = & \frac{1}{4}\rho_0 U^2 \int_h^H \delta'^3 dz - g \int_0^h (H - z)\rho_c(z) dz + \rho_B g h (H - \frac{h}{2}) \\ & + \frac{1}{2}\rho_0 U^2 (H - \frac{h}{2}) [1 - \delta'(h)]^2 + \frac{1}{4}\rho_0 U^2 h, \end{aligned} \quad (29)$$

where $\rho_a(0) = \rho_B$ is used. When ρ_c is assumed to be a constant, Eq. (29) is reduced to Eq. (4.8) of Reference [10]. According to Eqs. (22)–(24), the streamline displacement δ depends on the front speed U and the current height h , and when h is given the front speed U can be solved.

3 Gravity current of linearly stratified fluids

In this section, the current and the ambient fluid are assumed to be homogeneous or unstably stratified fluids with the linear density profiles:

$$\rho_c(z) = \rho_{CB} + (\rho_M - \rho_{CB}) \frac{z}{h}, \quad 0 \leq z \leq h, \quad (30)$$

$$\rho_a(z) = \rho_B + (\rho_T - \rho_B) \frac{z}{H}, \quad 0 \leq z \leq H. \quad (31)$$

In the following, we choose the density at the bottom of the far upstream ambient fluid as the reference density, i.e. $\rho_0 = \rho_B$. Substituting Eq. (31) into Eq. (22), we have

$$\delta''(z) = \frac{\beta^2}{H^2} \delta(z), \quad h < z \leq H, \quad (32)$$

where

$$\beta = \frac{1}{U} \sqrt{\frac{|\rho_T - \rho_B| g H}{\rho_B}} = \frac{\sqrt{S g' H}}{U} \quad (33)$$

according to Eqs. (5), (8), and (9).

3.1 Unstably stratified ambient fluid

In an unstably stratified ambient fluid with $0 < S \leq 1$ and $\rho_T > \rho_B$, the solution of Eq. (32) under the boundary conditions (23) and (24) is

$$\delta(z) = h \frac{\sinh[\beta(1 - z/H)]}{\sinh[\beta(1 - h/H)]}, \quad h \leq z \leq H. \quad (34)$$

It is noted that for stably stratified fluids, $\rho_T < \rho_B$, $-\beta^2$ instead of β^2 should be used in Eq. (32), and $\delta(z)$ is then expressed with trigonometric functions as in the previous study^[9].

Substituting Eqs. (30) and (34) into Eq. (29) and using Eqs. (5)–(9) and (33), we have

$$a^2 \gamma^2 \coth^2 \gamma + a(2-a)\gamma \coth \gamma + 1 - a - \frac{\gamma^2}{S} \frac{a}{1-a} [2 - a - S \frac{a^2}{3} - \sigma(1 - \frac{a}{3})] = 0, \quad (35)$$

where

$$a = \frac{h}{H}, \quad (36)$$

$$\gamma = \beta(1-a) = \frac{1-a}{U} \sqrt{\frac{Sg'h}{a}}. \quad (37)$$

For given non-dimensional current height a and stratification parameters S and σ , γ can be solved from Eq. (35), and then the Froude number is obtained as

$$Fr(a, S, \sigma) = \frac{1-a}{\gamma} \sqrt{\frac{S}{a}} \quad (38)$$

according to Eqs. (7) and (37).

3.2 homogeneous ambient fluid

For a homogeneous or an unstably stratified gravity current ($0 \leq \sigma \leq 1$) in a homogeneous ambient fluid ($S = 0$), we have $\beta = 0$ according to Eq. (33). The solution of Eq. (32) under the boundary conditions (23) and (24) is

$$\delta(z) = h \frac{H-z}{H-h}, \quad h \leq z \leq H. \quad (39)$$

Substituting Eq. (30), (39) and $\rho_a = \rho_B$ into Eq. (29) and using Eqs. (6)–(9), we have

$$Fr(a, 0, \sigma) = \sqrt{\frac{1-a}{1+a} [2 - a - \sigma(1 - \frac{a}{3})]}, \quad (40)$$

which is also a limiting case of Eq. (38) when $S \rightarrow 0$. Note that $\gamma \rightarrow 0$ when $S \rightarrow 0$ according to Eq. (37).

If the current is also homogeneous ($\sigma = 0$), then it follows from Eq. (40) that

$$Fr(a, 0, 0) = \sqrt{\frac{(1-a)(2-a)}{1+a}}, \quad (41)$$

which is consistent with the Benjamin theory^[1].

4 Numerical simulations and discussion

In order to verify the relationship between the front speed U and the current height h predicted by the inviscid theory, two-dimensional numerical simulations of the lock-exchange gravity current are carried out as shown in Fig. 2. The denser fluid

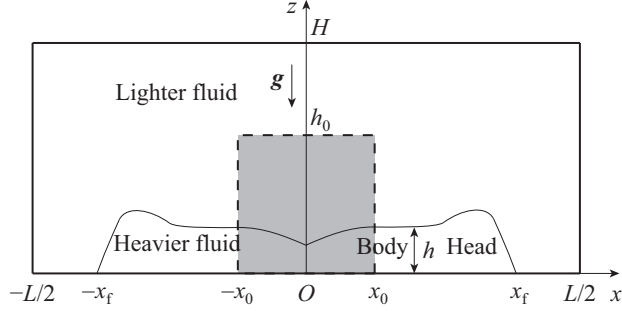


Figure 2: A schematic plot of the lock-exchange gravity current between free-slip walls. The shaded region is initially occupied by the denser fluid.

occupies initially a rectangular region with a length of $2x_0$ and a height of $h_0 \leq H$, where H is the distance between the free-slip walls. The length and height of the computational domain are L and H , respectively.

Introducing the non-dimensional coordinates, time, velocity, density, and pressure

$$(\tilde{x}, \tilde{z}) = \frac{(x, z)}{H}, \quad \tilde{t} = \frac{\nu}{H^2}t, \quad (\tilde{u}, \tilde{w}) = \frac{H}{\nu}(u, w), \quad \tilde{\rho} = \frac{\rho - \rho_0}{\rho_M - \rho_0}, \quad \tilde{p} = \frac{H^2}{\rho_0 \nu^2}(p + \rho_0 g z) \quad (42)$$

into Eqs. (1)–(4), we have the non-dimensional governing equations:

$$\frac{\partial \tilde{u}}{\partial \tilde{x}} + \frac{\partial \tilde{w}}{\partial \tilde{z}} = 0, \quad (43)$$

$$\frac{\partial \tilde{u}}{\partial \tilde{t}} + \tilde{u} \frac{\partial \tilde{u}}{\partial \tilde{x}} + \tilde{w} \frac{\partial \tilde{u}}{\partial \tilde{z}} = -\frac{\partial \tilde{p}}{\partial \tilde{x}} + \frac{\partial^2 \tilde{u}}{\partial \tilde{x}^2} + \frac{\partial^2 \tilde{u}}{\partial \tilde{z}^2}, \quad (44)$$

$$\frac{\partial \tilde{w}}{\partial \tilde{t}} + \tilde{u} \frac{\partial \tilde{w}}{\partial \tilde{x}} + \tilde{w} \frac{\partial \tilde{w}}{\partial \tilde{z}} = -\frac{\partial \tilde{p}}{\partial \tilde{z}} - Gr \tilde{\rho} + \frac{\partial^2 \tilde{w}}{\partial \tilde{x}^2} + \frac{\partial^2 \tilde{w}}{\partial \tilde{z}^2}, \quad (45)$$

$$\frac{\partial \tilde{\rho}}{\partial \tilde{t}} + \tilde{u} \frac{\partial \tilde{\rho}}{\partial \tilde{x}} + \tilde{w} \frac{\partial \tilde{\rho}}{\partial \tilde{z}} = \frac{1}{Sc} \left(\frac{\partial^2 \tilde{\rho}}{\partial \tilde{x}^2} + \frac{\partial^2 \tilde{\rho}}{\partial \tilde{z}^2} \right), \quad (46)$$

with

$$Gr = \frac{(\rho_M - \rho_0)gH^3}{\rho_0 \nu^2} = \frac{g'H^3}{\nu^2}, \quad (47)$$

where we have used $\rho_0 = \rho_B$ and Eqs. (8) and (9). The Schmidt number is $Sc = \nu/\kappa$ and is assumed to be 1 in the present simulations.

Equations (43)–(46) are solved with a pseudo-spectral method^[26] under the periodic boundary conditions in the horizontal direction. In the vertical direction, we assume the free-slip boundary conditions for the velocity and the zero-flux boundary condition for the density. The governing equations are discretized with 4096 Fourier modes and 257 Chebyshev polynomials in the horizontal and vertical directions, respectively. To achieve a high volume of release with $x_0 \gg h$ ^[27], we choose $\tilde{x}_0 = x_0/H = 4$ and $\tilde{L} = L/H = 16$. Note that the mode resolutions used in the x and z directions are 4 times and 1.25 times as large as those used in the previous study^[28], respectively, and it was checked that the front velocities obtained with half modes agreed with the present results to better than 3%.

Both fluids are at rest at $t = 0$. The initial density is

$$\tilde{\rho}(\tilde{x}, \tilde{z}, 0) = \begin{cases} 1 - \sigma + \sigma\tilde{z}/\tilde{h}_0, & |\tilde{x}| \leq \tilde{x}_0, 0 \leq \tilde{z} \leq \tilde{h}_0, \\ S\tilde{z}, & \text{elsewhere,} \end{cases} \quad (48)$$

where $\tilde{h}_0 = h_0/H$. The non-dimensional numerical front speed is defined as $\tilde{U} = UH/\nu = d\tilde{x}_f/d\tilde{t}$, where \tilde{x}_f is the abscissa of the intersection of the bottom wall and the isopycnal $\tilde{\rho} = (1 - \sigma)/2$ ^[29]. The Froude number is therefore $Fr = \tilde{U}/\sqrt{aGr}$ according to Eqs. (7), (36), and (47).

Based on the energy conservation for a steady current of inviscid homogeneous fluids ($S = \sigma = 0$), Benjamin proposed that the dimensionless current height is $a = 1/2$ ^[1]. Due to the velocity difference between the denser and lighter fluids near the interface, Kelvin-Helmholtz type instability may occur and the interfaces are mostly unstable. In addition, viscous dissipation will affect the current height as well. Consequently, different definitions were applied for the current height in the literature, e.g. the maximum height of the current head^[30], a temporal and spatial average over some distance behind the current head^[1, 14, 31]. Inspired by these previous studies, the non-dimensional numerical current height a for $S = \sigma = 0$ is defined as,

$$a = \frac{1}{\tilde{t}_2 - \tilde{t}_1} \int_{\tilde{t}_1}^{\tilde{t}_2} \frac{1}{\tilde{x}_d - \tilde{x}_u} \int_{\tilde{x}_u}^{\tilde{x}_d} \tilde{h} d\tilde{x} d\tilde{t}, \quad \tilde{h}(\tilde{x}, \tilde{t}) = \int_0^1 \tilde{\rho}(\tilde{x}, \tilde{z}, \tilde{t}) d\tilde{z}, \quad (49)$$

where \tilde{h} is the local current height, $\tilde{x}_u(\tilde{t})$ and $\tilde{x}_d(\tilde{t})$ are the most upstream and downstream positions where $\tilde{h} = \tilde{h}_0/2$, respectively, and $(\tilde{t}_1, \tilde{t}_2)$ is a period in the slumping phase. According to the above definition of a , Benjamin's solution $a = 1/2$ is recovered when $h_0 = H$ due to the symmetric property of the interface.

The contours of the density $\tilde{\rho}$ for different stratification cases at the same \tilde{t} , Gr , and \tilde{h}_0 are shown in Fig. 3, and the front speed is substantially affected by S and σ : increasing the unstably stratification parameter of the current σ decreases the front speed. It has been shown that Fr and h predicted by the steady and inviscid Benjamin theory are consistent generally with experiments^[32, 33] and numerical simulations^[34] for currents of homogeneous fluids. Considering the presence of interface mixing, these consistencies are striking^[33] and may be explained briefly as follows. Firstly, though the instabilities and mixing occur near the density interface following a current front, the far upstream is undisturbed and at the downstream position where $\tilde{h} = \tilde{h}_0/2$, e.g. \tilde{x} is about 3.3 in Fig. 3(a), the interface is not mixed. Consequently, the upstream and downstream boundary conditions still can be approximated by the inviscid model (Eq. (14)-(19)) during the slumping phase. Secondly, according to the experiments, the current front remains essentially unmixed during the slumping phase, and following the front there is a tail region near the bottom, which is almost unaffected by the mixing around the upper interface^[35, 36]. Similar phenomena can be observed in Fig. 3 as well. Thirdly, the characteristic current velocity ($\sqrt{g'h}$) is much faster than the diffusion ones (e.g. ν/h) for a current with small ν , and the error caused by ignoring the diffusion effects is limited during the slumping phase. Therefore, the inviscid theory does represent the basic mechanism governing the slumping phase, where the front velocity and the current height are assumed as constants.

The above arguments are applicable for both homogeneous fluids and stratified fluids when the unstably stratification is weak or before the unstably stratification leads to the Rayleigh-Bénard type convection and ruins the slumping phase.

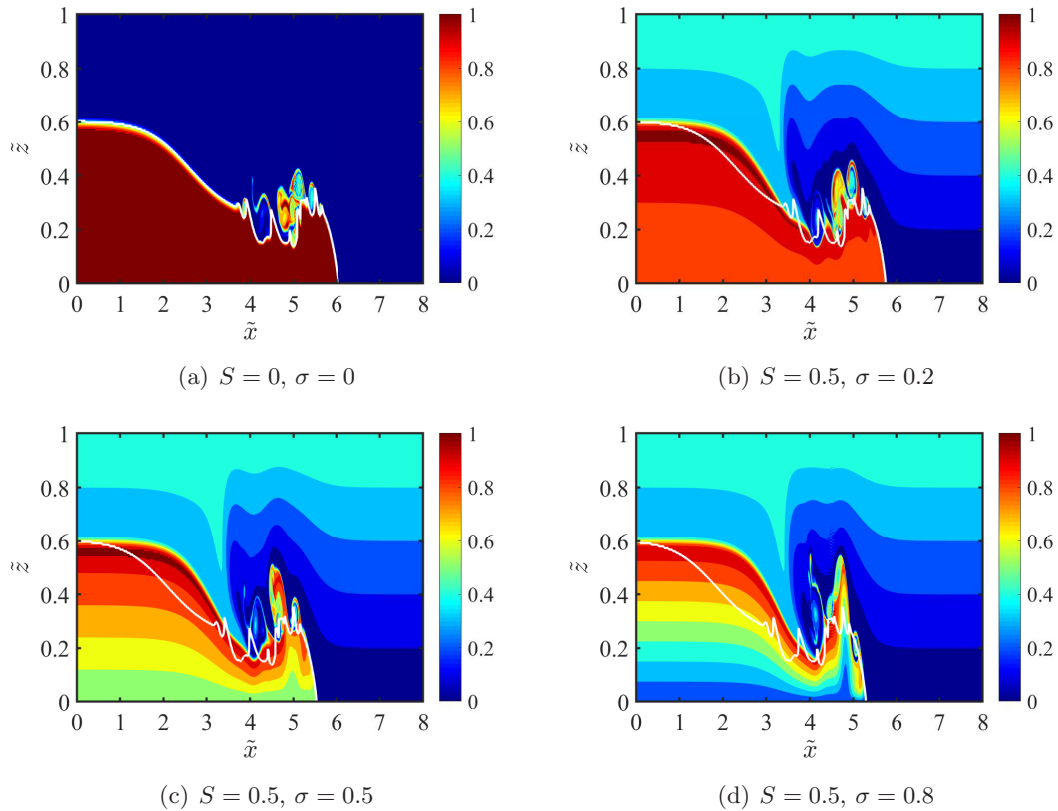


Figure 3: Contours of the density $\tilde{\rho}$ at $\tilde{t} = 10^{-4}$ in the numerical simulations with $Gr = 2 \times 10^9$ and $\tilde{h}_0 = 0.6$. The solid white curve shown in (a) indicates the local current height \tilde{h} , and is shifted accordingly in (b), (c), and (d) to fit the most downstream point of the current head.

According to the simulations shown in Fig. 3, the current interfaces for different stratified cases look similar as the solid white curves, which are the \tilde{h} curves for the homogeneous case (Fig. 3a), shifted to fit the front heads. Consequently, the entrainment characteristics of the present stratified cases are similar as those for homogeneous fluids. Because of the interface mixing and diffusion, \tilde{h} varies with time and the streamwise location, but its spatially averaged value does not change markedly during the slumping phase. Therefore, the current height a for a stratified case is set approximately the same value as that of a homogeneous case with the same Gr and h_0 .

Numerical simulations are carried out to test the inviscid relation between the Froude number Fr and the non-dimensional current height a (Eq. (38) and (40)). In order to diminish the viscous effect, the viscosity should be small or Gr should be large enough. As shown in Fig. 4, Fr increases with Gr at moderate Grashof numbers and remains nearly constant as $Gr > 10^9$. Therefore, $Gr = 2 \times 10^9$ is used in the following simulations, and the corresponding non-dimensional current heights for homogeneous fluids are $a = 0.27$ and 0.50 when the initial lock heights

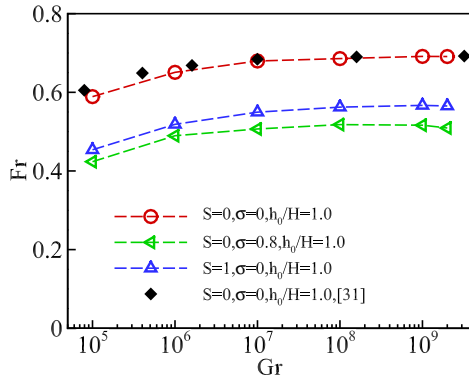


Figure 4: The Froude number Fr as a function of the Grashof number Gr in the numerical simulations. The hollow symbols represent the present numerical results, and the numerical results of [34] are shown as filled diamonds for reference.

are $\tilde{h}_0 = 0.6$ and 1, respectively.

According to the simulations, a is less than $\tilde{h}_0/2$ when $\tilde{h}_0 < 1$, and the corresponding Fr obtained with the Benjamin's theory (Eq. (41)) increases with the decrease of \tilde{h}_0 , illustrating the same trend as the simulations for the homogeneous fluids ($\sigma = S = 0$) as shown in Fig. 5(a). For stratified fluids, however, the Benjamin's theory is not applicable, because Fr becomes a decreasing function of S and σ . It is shown in Fig. 5 that for different S and σ , the present theoretical predictions shown by the solid lines agree with the simulation data, which are shown as symbols in Fig. 5. The stratification effects may be explained as follows. According to Eq. (48), the average density of the ambient fluid increases with S , while the average density of the current decreases with the increase of σ . Consequently, the increases of S and σ decrease the average density difference between the two fluids, and hence reduce the front speed and Fr . It is noted that when the unstable stratification is strong enough, Rayleigh-Bénard type convection will occur and the slumping period becomes shorter for stronger stratification. For very strong unstable stratifications, natural convection happens soon and the slumping phase is hard to exist.

5 Conclusions

The relation between the front speed and the current height of a gravity current at the slumping stage is analyzed with an inviscid theory for unstably stratified fluids, an extension of the Benjamin's theory^[1] for homogeneous fluids. In order to test the theoretical predictions, numerical simulations of lock-exchange gravity currents are carried out, and the Froude number Fr is found to increase with the Grashof number Gr when $Gr \leq 10^9$, reflecting the diffusion effects. At higher Grashof numbers, the Froude number becomes a weak function of Gr and mainly depends on the initial lock height \tilde{h}_0 and the stratification parameters S and σ . When the ambient fluid or the current is unstably stratified, the Froude numbers

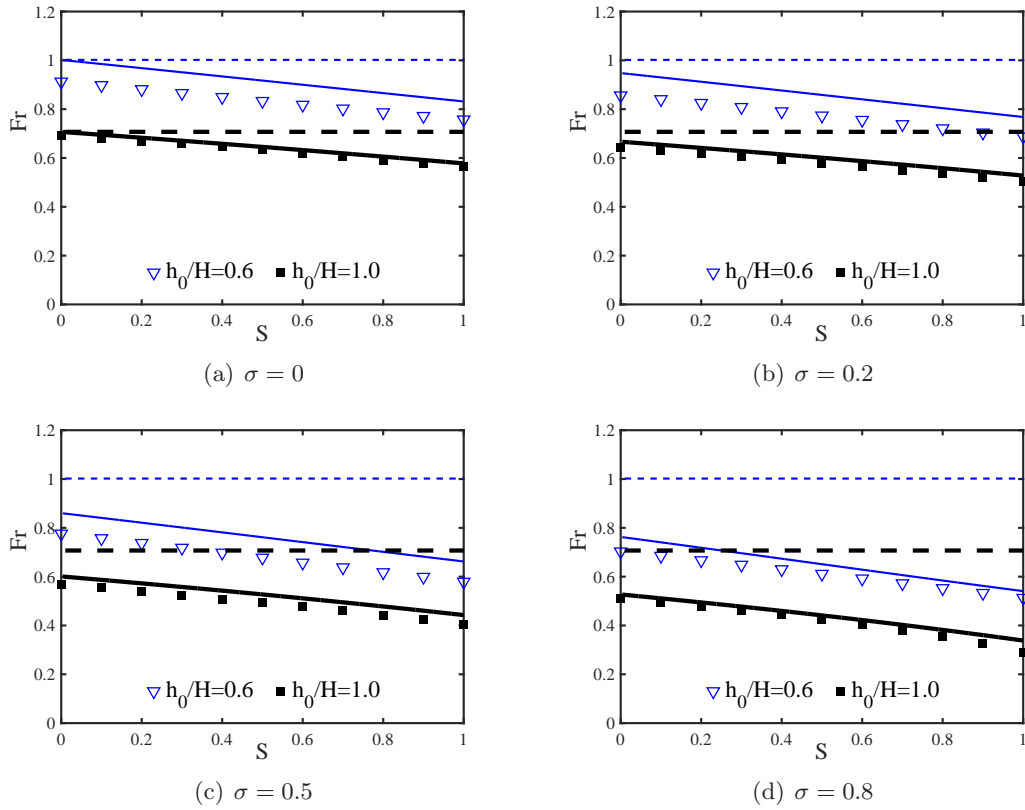


Figure 5: The Froude number Fr as a function of S , σ , and $\tilde{h}_0 = h_0/H$ at $Gr = 2 \times 10^9$. The symbols represent the numerical results. The solid and dashed lines represent the results of the present theory (Eq. (38)) and the Benjamin's theory^[1] (Eq. (41)), respectively.

obtained numerically deviate from the predictions of the Benjamin’s theory, but are consistent with the present theoretical values, indicating the substantial effect of stratification on the front speed and the current height. Though instabilities and the related mixing occur around the density interface, the consistency illustrates that the inviscid theory grasps the main mechanism governing the propagation of the gravity currents.

References

- [1] BENJAMIN, T. B. Gravity currents and related phenomena. *Journal of Fluid Mechanics*, **31**(2), 209–248 (1968)
- [2] SIMPSON, J. E. *Gravity Currents: In the Environment and the Laboratory*, 2nd ed., Cambridge University Press, Cambridge (1999)
- [3] MEIBURG, E. and KNELLER, B. Turbidity currents and their deposits. *Annual Review of Fluid Mechanics*, **42**, 135–156 (2010)
- [4] XIE, C.Y., TAO, J.J., and Zhang, L.S. Origin of lobe and cleft at the gravity current front. *Physical Review E*, **100**, 031103(R) (2019)
- [5] ZHANG, L.S., TAO, J.J., WANG, G.H., and ZHENG, X.J. Experimental study on the origin of lobe-cleft structures in a sand storm. *Acta Mechanica Sinica*, **37**, 47-52 (2021)
- [6] LOWE, R. J., ROTTMAN, J. W., and LINDEN, P. F. The non-Boussinesq lock-exchange problem. Part 1. Theory and experiments. *Journal of Fluid Mechanics*, **537**, 101–124 (2005)
- [7] SHIN, J. O., DALZIEL, S. B., and LINDEN, P. F. Gravity currents produced by lock exchange. *Journal of Fluid Mechanics*, **521**, 1–34 (2004)
- [8] MAURER, B. D., BOLSTER, D. T., and LINDEN, P. F. Intrusive gravity currents between two stably stratified fluids. *Journal of Fluid Mechanics*, **647**, 53–69 (2010)
- [9] UNGARISH, M. On gravity currents in a linearly stratified ambient: a generalization of Benjamin’s steady-state propagation results. *Journal of Fluid Mechanics*, **548**, 49–68 (2006)
- [10] WHITE, B. L. and HELFRICH, K. R. Gravity currents and internal waves in a stratified fluid. *Journal of Fluid Mechanics*, **616**, 327–356 (2008)
- [11] MAXWORTHY, T., LEILICH, J., SIMPSON, J. E., and MEIBURG, E. H. The propagation of a gravity current into a linearly stratified fluid. *Journal of Fluid Mechanics*, **453**, 371–394 (2002)
- [12] BRITTER, R. E. and SIMPSON, J. E. A note on the structure of the head of an intrusive gravity current. *Journal of Fluid Mechanics*, **112**, 459–466 (1981)
- [13] FAUST, K. M. and PLATE, E. J. Experimental investigation of intrusive gravity currents entering stably stratified fluids. *Journal of Hydraulic Research*, **22**(5), 315–325 (1984)
- [14] BORDEN, Z. and MEIBURG, E. Circulation based models for Boussinesq gravity currents. *Physics of Fluids*, **25**, 101301 (2013)
- [15] NASR-AZADANI, M. M. and MEIBURG, E. Gravity currents propagating into shear. *Journal of Fluid Mechanics*, **778**, 552–585 (2015)

- [16] NASR-AZADANI, M. M. and MEIBURG, E. Gravity currents propagating into ambients with arbitrary shear and density stratification: vorticity-based modelling. *Quarterly Journal of the Royal Meteorological Society*, **142**, 1359–1370 (2016)
- [17] KONOPLIV, N. A., LLEWELLYN SMITH, S. G., MCELWAIN, J. N., and MEIBURG, E. Modelling gravity currents without an energy closure. *Journal of Fluid Mechanics*, **789**, 806–829 (2016)
- [18] UNGARISH, M. and HUPPERT, H. E. On gravity currents propagating at the base of a stratified ambient. *Journal of Fluid Mechanics*, **458**, 283–301 (2002)
- [19] UNGARISH, M. Dam-break release of a gravity current in a stratified ambient. *European Journal of Mechanics B/Fluids*, **24**, 642–658 (2005)
- [20] UNGARISH, M. Gravity currents and intrusions of stratified fluids into a stratified ambient. *Environmental Fluid Mechanics*, **12**, 115–132 (2012)
- [21] GOLDMAN, R., UNGARISH, M., and YAVNEH, I. Gravity currents with double stratification: a numerical and analytical investigation. *Environmental Fluid Mechanics*, **14**, 471–499 (2014)
- [22] UNGARISH, M. Intrusive gravity currents in a stratified ambient: shallow-water theory and numerical results. *Journal of Fluid Mechanics*, **535**, 287–323 (2005)
- [23] KADER, B. A. and YAGLOM, A. M. Mean fields and fluctuation moments in unstably stratified turbulent boundary layers. *Journal of Fluid Mechanics*, **212**, 637–662 (1990)
- [24] LIU, C. H. and MONCRIEFF, M. W. An analytical study of density currents in sheared, stratified fluids including the effects of latent heating. *Journal of the Atmospheric Sciences*, **53**(22), 3303–3312 (1996)
- [25] LONG, R. R. Some aspects of the flow of stratified fluids: I. A theoretical investigation. *Tellus*, **5**(1), 42–58 (1953)
- [26] CHEVALIER, M., SCHLATTER, P., LUNDBLADH, A., HENNINGSON, D. S. SIMSON: A pseudo-spectral solver for incompressible boundary layer flows. *Tech. Rep. TRITA-MEK 2007:07*, Royal Institute of Technology, Stockholm, Sweden (2007).
- [27] CONSTANTINESCU, G. LES of lock-exchange compositional gravity currents: a brief review of some recent results. *Environmental Fluid Mechanics*, **14**, 295–317 (2014)
- [28] BONOMETTI, T., and BALACHANDAR, S. Effect of Schmidt number on the structure and propagation of density currents. *Theor. Comput. Fluid Dyn.*, **22**, 341–361 (2008)
- [29] BIRMAN, V. K., MEIBURG, E., and UNGARISH, M. On gravity currents in stratified ambients. *Physics of Fluids*, **19**, 086602 (2007)
- [30] SIMPSON, J. E., and BRITTER, R. E. The dynamics of the head of a gravity current advancing over a horizontal surface. *Journal of Fluid Mechanics*, **94**, 477–495 (1979).
- [31] BORDEN, Z., MEIBURG, E., and CONSTANTINESCU, G. Internal bores: an improved model via a detailed analysis of the energy budget. *Journal of Fluid Mechanics*, **703**, 279–314 (2012).
- [32] HUPPERT, H., and SIMPSON, J. E. The slumping of gravity currents. *Journal of Fluid Mechanics*, **99**, 785–799 (1980).

- [33] HACKER, J., LINDEN, P.F., and DALZIEL, S.B. Mixing in lock-release gravity currents. *Dynamics of Atmospheres and Oceans*, **24**, 183–195 (1996).
- [34] HÄRTEL, C., MEIBURG, E., and NECKER, F. Analysis and direct numerical simulation of the flow at a gravity-current head. Part 1. Flow topology and front speed for slip and no-slip boundaries. *Journal of Fluid Mechanics*, **418**, 189–212 (2000)
- [35] HALLWORTH, M. A., PHILLIPS, J. C., HUPPERT, H. E., and SPARKS, R.S.J. Entrainment in turbulent gravity currents. *Nature*, **362**, 829–831 (1993).
- [36] HALLWORTH, M. A., HUPPERT, H. E., PHILLIPS, J. C., and SPARKS, R.S.J. Entrainment into two-dimensional and axisymmetric turbulent gravity currents. *Journal of Fluid Mechanics*, **308**, 289–311 (1996).

Appendix A Streamline displacement equation

According to Eq. (12), the density is constant along each streamline, and therefore $\rho = \rho(\psi)$, where ψ is the stream function such that

$$u = -\frac{\partial\psi}{\partial z}, \quad (\text{A1})$$

$$w = \frac{\partial\psi}{\partial x}. \quad (\text{A2})$$

Without loss of generality, we require $\psi(x_r, 0) = 0$. Then we have

$$\psi(x_r, z) = Uz, \quad 0 \leq z \leq H \quad (\text{A3})$$

according to Eqs. (18) and (A1).

Eliminating the pressure in Eqs. (10) and (11) and using Eqs. (1) and (12), we have

$$u \frac{\partial f}{\partial x} + w \frac{\partial f}{\partial z} = 0, \quad (\text{A4})$$

where

$$f(x, z) = \frac{\partial u}{\partial z} - \frac{\partial w}{\partial x} - \frac{gz}{\rho_0} \frac{d\rho}{d\psi}. \quad (\text{A5})$$

The function $f(x, z)$ is therefore constant along each streamline.

For any point (x_1, z) in the ambient fluid ($h \leq z \leq H$) at the left boundary in Fig. 1, we define a streamline displacement $\delta(z)$ such that the points (x_1, z) and $(x_r, z - \delta(z))$ are on the same streamline. Consequently, we have $\rho(x_1, z) = \rho(x_r, z - \delta(z))$, and then

$$\rho_1(z) \equiv \rho(x_1, z) = \rho_a(z - \delta(z)), \quad h < z \leq H \quad (\text{A6})$$

according to Eq. (17).

Similarly, we have $f(x_1, z) = f(x_r, z - \delta(z))$, and then it follows from Eqs. (16), (18), and (19) that

$$\frac{du_1}{dz} = \frac{gz}{\rho_0} \frac{d\rho}{d\psi}(x_1, z) - \frac{g[z - \delta(z)]}{\rho_0} \frac{d\rho}{d\psi}(x_r, z - \delta(z)), \quad h < z \leq H. \quad (\text{A7})$$

As the stream function ψ is constant along each streamline, we have $\psi(x_1, z) = \psi(x_r, z - \delta(z))$, and then

$$u_1(z) \equiv u(x_1, z) = -U[1 - \delta'(z)], \quad h < z \leq H, \quad (\text{A8})$$

where $\delta' \equiv d\delta/dz$ and we have used Eqs. (A1) and (A3). Note that u_1 and ρ_1 may not be continuous at the interface $z = h$ according to Eqs. (14), (15), (A6), and (A8).

It is straightforward to examine that $d\rho/d\psi$ is also constant along each streamline. As a result,

$$\frac{d\rho}{d\psi}(x_1, z) = \frac{d\rho}{d\psi}(x_r, z - \delta(z)), \quad h < z \leq H. \quad (\text{A9})$$

Furthermore, we have

$$\frac{d\rho}{d\psi}(x_r, z - \delta(z)) = \frac{1}{U} \frac{d\rho_a}{dz}|_{z-\delta(z)}, \quad h < z \leq H \quad (\text{A10})$$

according to Eqs. (17) and (A3).

Substituting Eqs. (A8)–(A10) into Eq. (A7), we have

$$\delta''(z) = \frac{g}{\rho_0 U^2} \frac{d\rho_a}{dz}|_{z-\delta(z)} \delta(z), \quad h < z \leq H, \quad (\text{A11})$$

where $\delta'' \equiv d^2\delta/dz^2$. The boundary conditions are

$$\delta(h) = h, \quad (\text{A12})$$

$$\delta(H) = 0. \quad (\text{A13})$$

Eq. (A11) seems a simplified version of Long's model^[25], but it should be noted that ρU^2 is required to be constant in the far upstream flow in Long's model, an inapplicable assumption for a stratified ambient fluid with a uniform velocity. As shown above, this requirement is circumvented by the Boussinesq approximation in this paper.